IAI Journals.ASM.org

Role of Ferric Reductases in Iron Acquisition and Virulence in the Fungal Pathogen *Cryptococcus neoformans*

Sanjay Saikia, Debora Oliveira, Guanggan Hu, James Kronstad

Michael Smith Laboratories, Department of Microbiology and Immunology, and Faculty of Land and Food Systems, The University of British Columbia, Vancouver, British Columbia, Canada

Iron acquisition is critical for the ability of the pathogenic yeast *Cryptococcus neoformans* to cause disease in vertebrate hosts. In particular, iron overload exacerbates cryptococcal disease in an animal model, defects in iron acquisition attenuate virulence, and iron availability influences the expression of major virulence factors. *C. neoformans* acquires iron by multiple mechanisms, including a ferroxidase-permease high-affinity system, siderophore uptake, and utilization of both heme and transferrin. In this study, we examined the expression of eight candidate ferric reductase genes and their contributions to iron acquisition as well as to ferric and cupric reductase activities. We found that loss of the *FRE4* gene resulted in a defect in production of the virulence factor melanin and increased susceptibility to azole antifungal drugs. In addition, the *FRE2* gene was important for growth on the iron sources heme and transferrin, which are relevant for proliferation in the host. Fre2 may participate with the ferroxidase Cfo1 of the high-affinity uptake system for growth on heme, because a mutant lacking both genes showed a more pronounced growth defect than the *fre2* single mutant. A role for Fre2 in iron acquisition is consistent with the attenuation of virulence observed for the *fre2* mutant. This mutant also was defective in accumulation in the brains of infected mice, a phenotype previously observed for mutants with defects in high-affinity iron uptake (e.g., the *cfo1* mutant). Overall, this study provides a more detailed view of the iron acquisition components required for *C. neoformans* to cause cryptococcosis.

Iron is an essential element for almost all organisms, due to its role in various metabolic processes. However, its bioavailability in the environment is extremely limited because it is rapidly oxidized in the presence of atmospheric oxygen to insoluble ferric hydroxides. In addition, available iron in mammals is also severely limited because it is in heme-containing proteins and bound to extracellular carrier proteins, such as transferrin and lactoferrin, as well as to the intracellular storage protein ferritin. To overcome this challenge of limited iron availability, pathogens have evolved multiple mechanisms to acquire iron from the environment and from within the mammalian host. These include a reductive high-affinity uptake system, the production and uptake of siderophores, which are low-molecular-weight iron chelators that have a high affinity specifically for ferric iron, and the use of both heme and transferrin.

Fungal pathogens of humans employ different iron acquisition mechanisms that are likely to be important virulence determinants. For example, siderophores play an important role both in iron acquisition and in virulence for the invasive mold *Aspergillus fumigatus* (1–3). Although the pathogenic yeasts *Cryptococcus neoformans* and *Candida albicans* are not known to produce their own siderophores, they have siderophore transporters that are employed to obtain iron from siderophores produced by other organisms (4, 5). However, siderophore iron uptake does not appear to be important in the virulence of these two pathogens. In addition, both *C. neoformans* and *C. albicans* are able to utilize heme as an iron source. The cell wall mannoproteins Cig1 (in *C. neoformans*) and Rbt5 and Rbt51 (in *C. albicans*), as well as the heme oxygenase Hmx1 (in *C. albicans*), are involved in acquiring iron from heme (6–11). The reductive high-affinity iron uptake system is an important virulence determinant in *C. neoformans* and *C. albicans* but not in *A. fumigatus*, and this mechanism is employed by these two pathogens to acquire iron from transferrin in mammalian hosts (7, 8, 12). This iron uptake system involves the reduction of ferric iron to ferrous iron by cell surface reductases, followed by ferrous iron oxidation by a ferroxidase coupled to an iron permease for transport. Since the iron must be reduced before it becomes a substrate for the ferroxidase-permease complex, enzymatic and/or nonenzymatic ferric reductase activity is critically required for iron acquisition through the reductive uptake system. Therefore, the candidate genes encoding these enzymes in *C. neoformans* are the focus of the study reported in this article.

Ferric reductases are integral membrane proteins that require NADPH, flavin mononucleotide (FMN), and heme for activity. They catalyze the oxidation of cytoplasmic NADPH and transfer the electron across the plasma membrane to reduce metals like iron and copper. For fungi, these reductases have been studied extensively in *Saccharomyces cerevisiae* and also in *C. albicans*, *Schizosaccharomyces pombe*, and *A. fumigatus* (12–17). The number of ferric reductases varies across the fungi, with 8 in *S. cerevisiae*, 2 in *S. pombe*, 16 in *C. albicans*, and 15 in *A. fumigatus*. In *S. cerevisiae*, Fre1 and Fre2 account for the majority of the cell surface ferric reductase activity. These reductases also have cupric reductase activity and are able to facilitate the use of siderophore-bound iron (18, 19). Fre3 and Fre4 from *S. cerevisiae* are also able

Received 22 October 2013 **Returned for modification** 13 November 2013
Accepted 2 December 2013
Published ahead of print 9 December 2013
Editor: G. S. Deepe, Jr.
Address correspondence to James Kronstad, kronstad@msl.ubc.ca.
Supplemental material for this article may be found at http://dx.doi.org/10.1128/IAI.01357-13.

doi:10.1128/IAI.01357-13

TABLE 1 Strains used in this study

Strain	Description	Source
H99	*C. neoformans* wild-type strain	J. Heitman
*fre1*Δ mutant	*fre1* deletion mutant	This study
*fre2*Δ mutant	*fre2* deletion mutant	This study
*fre2*Δ + *FRE2* complemented strain	*FRE2* complemented strain	This study
*fre3*Δ mutant	*fre3* deletion mutant	This study
*fre4*Δ mutant	*fre4* deletion mutant	This study
*fre4*Δ + *FRE4* complemented strain	*FRE4* complemented strain	This study
*fre5*Δ mutant	*fre5* deletion mutant	This study
*fre6*Δ mutant	*fre6* deletion mutant	This study
*fre7*Δ mutant	*fre7* deletion mutant	This study
*fre201*Δ mutant	*fre201* deletion mutant	This study
*fre2*Δ *fre4*Δ mutant	*fre2 fre4* double deletion mutant	This study
*fre2*Δ *fre4*Δ + *FRE2* complemented strain	*FRE2* complemented in *fre2 fre4* double deletion mutant	This study
*fre2*Δ *fre4*Δ + *FRE4* complemented strain	*FRE4* complemented in *fre2 fre4* double deletion mutant	This study
301 D8	T-DNA insertion mutant of *FRE2* in *cfo1* deletion background	35

to catalyze the reductive release of iron from siderophores (19). The expression of the genes encoding these reductases and also Fre5 and Fre6 is induced by iron depletion. The transcription of *FRE1* and *FRE7* is also induced by copper depletion (18, 20, 21). In *C. albicans*, Fre10 and Fre7 are the major ferric reductases, and they also have cupric reductase activity (12, 15, 22). The genes encoding these and other reductases respond to a wide range of environmental conditions, including iron depletion (23, 24). The *S. pombe* ferric reductase Frp1 is essential for reductive iron uptake and is transcriptionally repressed by iron (17). In *A. fumigatus*, a role for FreB in iron acquisition via the reductive uptake system has been demonstrated (13). Although all of these studies implicated their respective ferric reductases in iron acquisition, no role in virulence was observed in *A. fumigatus* and *C. albicans*.

The *C. neoformans* genome encodes eight putative metallo/ferric reductases (hence called "ferric reductases"). In this study, we examined the expression of these genes in response to iron limitation and constructed deletion mutants of all eight reductases to begin to analyze their roles in iron acquisition. We found that Fre2 is required for growth on hemin and transferrin as the sole iron sources and that Fre4 has a role in melanin production and resistance to azole drugs. The genes coding for these two proteins also had a shared pattern of regulation that was distinct from that of the other six genes. We therefore focused the bulk of our analyses on Fre2 and Fre4 and demonstrated that mutants lacking *FRE2* alone or both *FRE2* and *FRE4* were attenuated for virulence in a mouse model of cryptococcosis.

MATERIALS AND METHODS

Strains and growth assays. The *C. neoformans* variety *grubii* strains used in this study are listed in Table 1. All strains were maintained on YPD medium (1% yeast extract, 2% peptone, 2% glucose). Yeast nitrogen base low-iron medium (YNB-LIM) (YNB [pH 7.2] plus 150 μM bathophenanthroline disulfonate [BPS]) and defined low-iron medium (LIM) were prepared as described previously (7, 25, 26) and used as iron-limiting media, supplemented as indicated, for phenotypic characterization. YNB low-copper medium (YNB-LCM) (YNB [pH 7.2] plus 100 μM bathocuproine disulfonate [BCS]) was prepared similarly to YNB-LIM. Defined low-copper medium (LCM) was also prepared similar to defined LIM, except that $CuSO_4$ was omitted and $FeCl_3$ was added. Cells were starved for iron or copper by growing in the respective limiting media at 30°C for 2 days. For growth assays in liquid media, a final concentration of 5×10^4 cells ml^{-1} was inoculated in the medium with or without supplemented iron sources. Cells were incubated at 30°C, and growth was monitored by measuring the optical density at 600 nm. For growth assays on solid media, 10-fold serial dilutions of cells were spotted on agar plates with or without supplemented iron sources. Plates were incubated at 30°C for 2 days before being photographed. Growth of the strains was also assessed by a high-throughput 96-well microplate assay using the Infinite M200 PRO plate reader (Tecan, Austria). For this assay, iron-starved cells were inoculated in 200 μl of YNB-LIM with or without supplemented iron sources for 3 to 4 days at 30°C (final inoculum of 10^4 cells). Growth was monitored by measuring optical density at 600 nm, and the resulting data were analyzed using the Magellan software (Tecan, Austria).

Construction of deletion and complemented strains. All deletion mutants were constructed by homologous recombination using gene-specific knockout cassettes, which were amplified by three-step overlapping PCR (27, 28) with the primers listed in Table S1 in the supplemental material. All three antibiotic resistance markers, namely the resistance markers for nourseothricin (*NAT*), neomycin (*NEO*), and hygromycin (*HYG*), were amplified by PCR using the primers M13-F and M13-R and the plasmids pCH233, pJAF1, and pJAF15, respectively, as the templates. In general, the gene-specific knockout primers 1 and 2 and 3 and 4 were used to amplify the flanking sequences of their respective genes; and the nested knockout primers 5 and 6 were used to amplify the gene-specific deletion construct containing the resistance marker. Primers 2 and 3 were chimeric primers containing a 30-bp sequence at their 5′ end that was complementary to the sequence from resistance markers to facilitate overlap during PCR. All constructs for deletions or complementation were introduced into the H99 wild-type (WT) strain or into the *fre2*Δ or *fre4*Δ mutants, by biolistic transformation, as described previously (29).

To construct the *fre1*Δ mutant, a deletion cassette was constructed by PCR using primers H07770-ko-1, H07770-ko-2, H07770-ko-3, H07770-ko-4, H07770-ko-5, and H07770-ko-6, with H99 genomic DNA and the plasmid pJAF15 as the templates. The 3.31-kb open reading frame of *FRE1* was replaced with the 2.09-kb *HYG* cassette using 5′ and 3′ flanking sequences of *FRE1*. Positive transformants were identified by PCR and confirmed by Southern blotting.

To construct the *fre2*Δ mutant, a deletion cassette was constructed by PCR using primers H06821-ko-1, H06821-ko-2, H06821-ko-3, H06821-ko-4, H06821-ko-5, and H06821-ko-6, with H99 genomic DNA and the plasmid pCH233 as the templates. The 2.38-kb open reading frame of *FRE2* was replaced with the 1.65-kb *NAT* cassette using 5′ and 3′ flanking sequences of *FRE2*. Positive transformants were identified by PCR and confirmed by Southern blotting. To construct the *fre2*Δ + *FRE2* complemented strain, a complementation construct containing the *FRE2* gene and *HYG* resistance marker was generated by cloning. A 0.84-kb DNA fragment downstream of the *FRE2* translation stop site was PCR amplified using primers H06821C-Sp and H06821C-Hi with the introduction of the SpeI restriction enzyme site, with genomic DNA as the template. The amplified 0.84-kb DNA fragment was digested with HindIII/SpeI and ligated with pJAF15 to construct pHYGFRE2L. A 3.24-kb DNA fragment containing the *FRE2* gene, along with the promoter and terminator regions, was PCR amplified using primers H06821C-Xb and H06821C-No with the introduction of XbaI and NotI restriction enzyme sites, with genomic DNA as the template. The amplified 3.24-kb DNA fragment was digested with XbaI/NotI and ligated with pHYGFRE2L to construct pSS117. This plasmid was linearized with XbaI and introduced into the *fre2*Δ mutant.

To construct the *fre3*Δ mutant, a deletion cassette was constructed by PCR using primers H06524-ko-1, H06524-ko-2, H06524-ko-3, H06524-

ko-4, H06524-ko-5, and H06524-ko-6, with H99 genomic DNA and the plasmid pJAF1 as the templates. The 2.50-kb open reading frame of *FRE3* was replaced with the 1.86-kb *NEO* cassette using 5′ and 3′ flanking sequences of *FRE3*. The resulting transformants were screened and confirmed by PCR.

To construct the *fre4*Δ mutant, a deletion cassette was constructed by PCR using primers H07334-ko-1, H07334-ko-2, H07334-ko-3, H07334-ko-4, H07334-ko-5, and H07334-ko-6, with H99 genomic DNA and plasmid pJAF1 as the templates. The 2.35-kb open reading frame of *FRE4* was replaced with the 1.86-kb *NEO* cassette using 5′ and 3′ flanking sequences of *FRE4*. Positive transformants were identified by PCR and confirmed by Southern blotting. To construct the *fre4*Δ + *FRE4* complemented strain, a complementation construct containing the *FRE4* gene and *HYG* resistance marker was generated by cloning. A 0.87-kb DNA fragment downstream of the *FRE4* translation stop site was PCR amplified using primers H07334C-Sp and H07334C-Hi with the introduction of SpeI restriction enzyme site, with genomic DNA as the template. The amplified 0.87-kb DNA fragment was digested with HindIII/SpeI and ligated with pJAF15 to construct pHYGFRE4L. A 3.65-kb DNA fragment containing the *FRE4* gene, along with the promoter and terminator regions, was PCR amplified using primers H07334C-Xb and H07334C-No with the introduction of XbaI and NotI restriction enzyme sites, with genomic DNA as the template. The amplified 3.65-kb DNA fragment was digested with XbaI/NotI and ligated with pHYGFRE4L to construct pSS118. This plasmid was linearized with XbaI and introduced into the *fre4*Δ mutant.

To construct the *fre5*Δ mutant, a deletion cassette was constructed by PCR using primers H07604-ko-1, H07604-ko-2, H07604-ko-3, H07604-ko-4, H07604-ko-5, and H07604-ko-6, with H99 genomic DNA and the plasmid pJAF1 as the templates. The 2.29-kb open reading frame of *FRE5* was replaced with the 1.86-kb *NEO* cassette using 5′ and 3′ flanking sequences of *FRE5*. The resulting transformants were screened and confirmed by PCR.

To construct the *fre6*Δ mutant, a deletion cassette was constructed by PCR using primers H06976-ko-1, H06976-ko-2, H06976-ko-3, H06976-ko-4, H06976-ko-5, and H06976-ko-6, with H99 genomic DNA and the plasmid pCH233 as the templates. The 1.71-kb open reading frame of *FRE6* was replaced with the 1.65-kb *NAT* cassette using 5′ and 3′ flanking sequences of *FRE6*. The resulting transformants were screened and confirmed by PCR.

To construct the *fre7*Δ mutant, a deletion cassette was constructed by PCR using primers H00876-ko-1, H00876-ko-2, H00876-ko-3, H00876-ko-4, H00876-ko-5, and H00876-ko-6, with H99 genomic DNA and the plasmid pJAF1 as the templates. The 2.24-kb open reading frame of *FRE7* was replaced with the 1.86-kb *NEO* cassette using 5′ and 3′ flanking sequences of *FRE7*. The resulting transformants were screened and confirmed by PCR.

To construct the *fre201*Δ mutant, a deletion cassette was constructed by PCR using primers H03498-ko-1, H03498-ko-2, H03498-ko-3, H03498-ko-4, H03498-ko-5, and H03498-ko-6, with H99 genomic DNA and the plasmid pCH233 as the templates. The 2.36-kb open reading frame of *FRE201* was replaced with the 1.65-kb *NAT* cassette using 5′ and 3′ flanking sequences of *FRE201*. The resulting transformants were screened and confirmed by PCR.

To construct the *fre2*Δ *fre4*Δ double mutant, the *FRE2*-specific deletion cassette (described above) was introduced into the *fre4*Δ strain (described above) by biolistic transformation. Positive transformants were identified by PCR and confirmed by Southern blotting. To construct the *fre2*Δ *fre4*Δ + *FRE2* and *fre2*Δ *fre4*Δ + *FRE4* complemented strains, the linearized plasmids pSS17 (*FRE2*) and pSS118 (*FRE4*) (described above), respectively, were introduced into the *fre2*Δ *fre4*Δ double mutant. The resulting transformants were screened and confirmed by PCR.

Real-time qRT-PCR. Real-time quantitative reverse transcription-PCR (qRT-PCR) was performed as follows. To examine gene expression, three biological replicates of the WT and *fre4*Δ mutant strains were grown in 5 ml of YPD medium overnight at 30°C. Cells were washed twice in Chelex-treated water followed by growth in YNB-LIM or YNB-LCM for 2 days to starve the cells for iron or copper, respectively. Cells were then washed and grown either in 5 ml YNB-LIM (with or without 100 μM $FeCl_3$ and 10 μM hemin) or in 5 ml YNB-LCM (with or without 100 μM $CuSO_4$) for 6 h at 30°C (final density of 10^7 cells ml^{-1}). Total RNA was extracted and cDNA was synthesized as described previously (30). Relative gene expression was quantified based on the threshold cycle ($2^{-\Delta\Delta CT}$) method (31). 18S rRNA was used as an internal control for normalization.

Ferric and cupric reductase assays. Ferric and cupric reductase activities were measured as described previously (32). Briefly, cells grown overnight in YPD medium were starved for iron or copper in defined LIM or defined LCM, respectively. The iron- or copper-starved cells were then grown in defined LIM or defined LCM with or without 100 μM $FeCl_3$ or 100 μM $CuSO_4$, respectively, for 6 h. For the ferric reductase assay (in a total volume of 2 ml), 1 ml of cells was mixed with BPS and Fe(III)-Na EDTA (1 mM each), and the mixture was incubated for 1 h in the dark before the A_{535} (ε = 22,140 M^{-1} cm^{-1}) of the colored Fe(II)-BPS complex was read. Similarly for the cupric reductase assay, 1 ml of cells was mixed with BCS and $CuSO_4$ (1 mM each), and the Cu reductase activity was measured by reading the A_{478} (ε = 9,058 M^{-1} cm^{-1}) of the colored Cu(I)-BCS complex.

Noniron metalloporphyrin uptake assay. Cells grown overnight in YPD medium were starved for iron in YNB-LIM. YPD or YNB-LIM plates with or without 10 μM hemin or 100 μM $FeCl_3$ were spread with 200 μl of 10 μM Ga-PPIX (Frontier Scientific), 10 μM Mn-PPIX (Frontier Scientific), or 10 μM $GaCl_3$ (Sigma-Aldrich) and then were spotted with 10-fold serial dilutions of the cells. The plates were incubated for 2 days at 30°C before being photographed.

Melanin assay. Melanin production was examined on L-3,4-dihydroxyphenylalanine (L-DOPA) agar plates containing 0.1% glucose.

Virulence assay. The virulence of cryptococcal strains was examined in an inhalation model of cryptococcosis using female BALB/c mice (4 to 6 weeks old) from Charles River Laboratories (Senneville, Ontario, Canada), as described previously (30). Briefly, cells grown overnight in YPD medium were washed twice and resuspended in phosphate-buffered saline (PBS) (Invitrogen, Canada). The BALB/c mice were intranasally inoculated with a suspension of 10^4 cells in 50 μl. The health status of the mice was monitored daily after inoculation. Mice that showed disease symptoms and reached 15% weight loss were euthanized by CO_2 anoxia. Statistical analyses of survival differences were performed by log rank tests using GraphPad Prism software (San Diego, CA). The fungal loads in the organs of three mice from each group were determined as described previously (30). The protocol for the virulence assay (protocol A13-0093) was approved by the University of British Columbia Committee on Animal Care. For histopathology studies, the lungs from three euthanized mice from each group were fixed in 10% neutral buffered formalin. The tissue was then embedded in paraffin and cut into 5-μm-thick sections, stained with hematoxylin and eosin (H&E) or Mayer's mucicarmine (MM), and then fixed on slides. Slides were examined by light microscopy under 5× objective magnification.

RESULTS

The *C. neoformans* genome encodes eight putative ferric reductases. We previously found that two iron regulators, the GATA factor Cir1 and the regulatory subunit HapX of the CCAAT-binding complex, both influenced the expression of a set of genes encoding predicted ferric reductases under iron-limiting conditions (30). This regulation suggested a role for these putative ferric reductases in iron acquisition. Therefore, we searched the *C. neoformans* genome by BLAST to identify genes corresponding to homologues of the *S. cerevisiae* ferric reductases as part of the present study, and this analysis identified eight candidates. The proteins encoded by these genes contained characteristic features of ferric reductases, including a flavin adenine dinucleotide (FAD)-binding do-

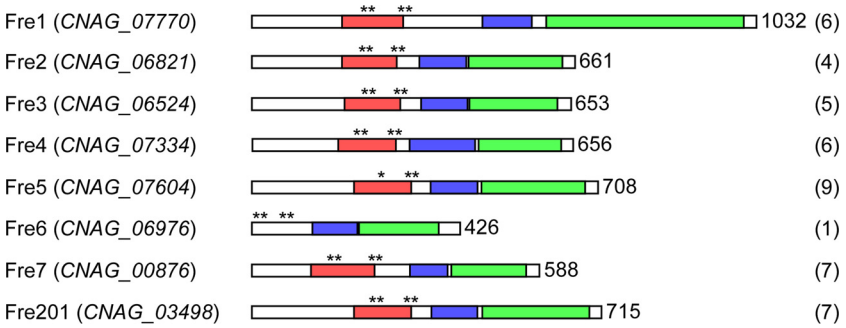

FIG 1 Domain structure of *C. neoformans* ferric reductases. Colored boxes indicate the ferric reductase transmembrane component-like domain (red box), the flavin adenine dinucleotide (FAD)-binding domain (blue box), and the ferric reductase NAD-binding domain (green box). An asterisk indicates the *bis*-heme motif comprising four conserved histidine residues. The length in number of amino acids is indicated adjacent to the sequences. Numbers in parentheses indicate the number of transmembrane regions.

main (IPR013112/PF08022), a ferric reductase NAD-binding domain (IPR013121/PF08030), and a ferric reductase transmembrane component-like domain (IPR013130/PF01794) (Fig. 1). However, the ferric reductase transmembrane domain was not present in the predicted polypeptide encoded by CNAG_06976.7. We named the corresponding genes based on their closest similar orthologues in the *S. cerevisiae* genome database *viz. FRE1* (CNAG_07770.7), *FRE2* (CNAG_06821.7), *FRE3* (CNAG_06524.7), *FRE4* (CNAG_07334.7), *FRE5* (CNAG_07604.7), *FRE6* (CNAG_06976.7), and *FRE7* (CNAG_00876.7). Although the top hit for CNAG_03498.7 in *S. cerevisiae* (Fre2) was more similar to the product encoded by CNAG_06821.7, we named the gene corresponding to CNAG_03498.7 "*FRE201*" to reflect the relationship to *FRE2*. These putative ferric reductases contained four to nine transmembrane regions, except that Fre6 contained only one transmembrane region. In addition, four conserved histidine residues that have a role in heme coordination were present in all of the candidate ferric reductases except Fre5. The first canonical heme-spanning histidine in this reductase was replaced by an arginine residue that is highly conserved in bacterial ferric reductases (33). Comparisons of the identities and similarities of the amino acid sequences of the eight ferric reductases are shown in Table S2 in the supplemental material.

Expression of the *FRE* genes is iron and copper responsive. In *S. cerevisiae* and other microorganisms, the expression of *FRE* genes is transcriptionally regulated by iron and/or copper availability. In a previous microarray study, we found that a subset of the putative cryptococcal ferric reductases was transcriptionally regulated by iron and that this regulation was mediated, at least in part, by the transcription factors Cir1 and HapX (30). To validate and extend this analysis, we studied the expression of all eight putative ferric reductases in response to iron or copper availability during growth. The wild-type (WT) strain was grown either in YNB low-iron medium (YNB-LIM) without or with 100 μM $FeCl_3$ or 10 μM hemin or in YNB low-copper medium (YNB-LCM) without or with 100 μM $CuSO_4$ for 6 h, and the expression of *FRE* genes was analyzed by real-time qRT-PCR. The transcript levels of the *FRE2* and *FRE4* genes were reduced in the presence of both $FeCl_3$ and hemin (Fig. 2A). This result suggests that the proteins encoded by these genes have a role in iron acquisition under iron-limited conditions, likely through a contribution to the high-affinity iron uptake system. However, all of the other *FRE* genes (*FRE1*, *FRE3*, *FRE5*, *FRE6*, *FRE7*, and *FRE201*) showed differential regulation depending upon the iron source. In particular, the transcripts of most of these genes, particularly *FRE3*, *FRE5*, and *FRE7*, were increased in the presence of hemin. However, the presence of $FeCl_3$ had only a moderate repressive effect on the expression of these *FRE* genes. In the presence of copper, the transcript levels of the *FRE2* to *-5*, *FRE7*, and *FRE201* genes were reduced, with *FRE4* showing the greatest reduction (Fig. 2B). The results for these genes may suggest roles in copper metabolism. In contrast, the expression of the *FRE1* and *FRE6* genes was elevated under high-copper conditions, with a particularly robust response observed for *FRE6*.

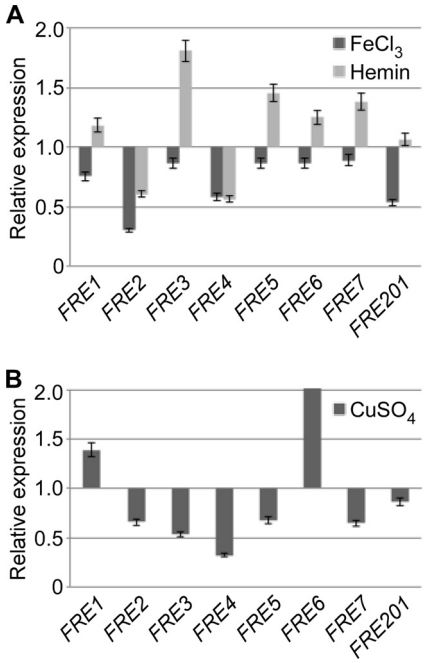

FIG 2 Expression analysis of *C. neoformans FRE* transcript levels. (A) Relative expression of *FRE* genes in the WT strain in the presence of iron, as examined by qRT-PCR. RNA was extracted from cells incubated in YNB-LIM with no iron or with either 100 μM $FeCl_3$ or 10 μM hemin for 6 h. (B) Relative expression of *FRE* genes in the WT strain in the presence of copper, as examined by qRT-PCR. RNA was extracted from cells incubated in YNB-LCM with no copper or with 100 μM $CuSO_4$ for 6 h. The data were normalized using 18S rRNA as an internal control. The data are from three biological replicates, and the bars represent standard errors.

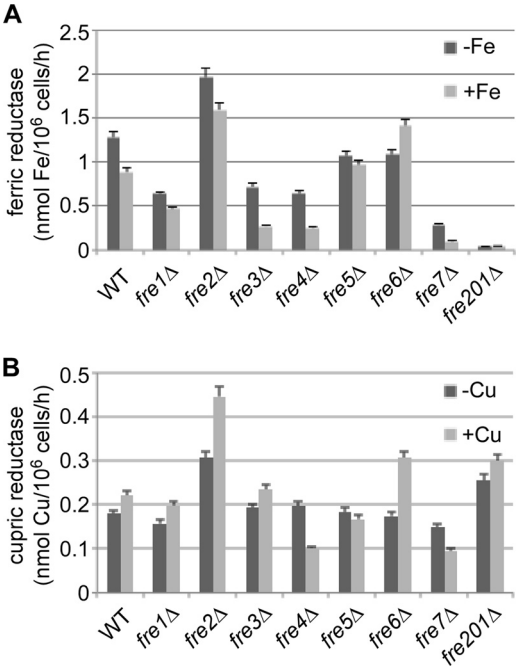

FIG 3 Reductase activities of *fre*Δ mutants. (A) Ferric reductase activity of WT and *fre*Δ mutant strains grown in defined LIM with no iron (−Fe) or with 100 μM $FeCl_3$ (+Fe). (B) Cupric reductase activity of WT and *fre*Δ mutant strains grown in defined LCM with no copper (−Cu) or with 100 μM $CuSO_4$ (+Cu). The data are from three replicates, and the bars represent standard errors.

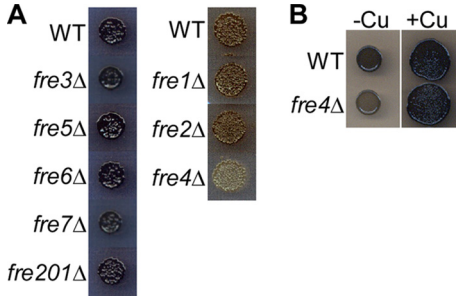

FIG 4 The *fre4*Δ mutant is defective in melanin production. (A) Melanin production in WT and *fre*Δ mutant strains was compared by growing cells on L-DOPA plates for 2 days. (B) Melanin production in the *fre4*Δ mutant was restored to the WT level by addition of exogenous copper. Cells were grown on L-DOPA plates with no $CuSO_4$ (−Cu) or with 50 μM $CuSO_4$ (+Cu) for 2 days.

Ferric and cupric reductase activities of *FRE* deletion strains. We next constructed deletion mutants in the WT background to characterize the functions of each *FRE* gene, including their contribution in reducing ferric and/or cupric ion to the ferrous and/or cuprous forms. Two independent mutants for each gene were subsequently used in all phenotypic analyses, and the data are shown here for only one representative independent mutant for each gene. In addition, the *fre2*Δ and *fre4*Δ mutations were complemented with the WT genes as described below. For ferric ion reduction, the WT and *fre*Δ deletion strains were grown in defined LIM without or with 100 μM $FeCl_3$. In the absence of iron, the ferric reductase activity in all of the *fre*Δ mutants, except *fre2*Δ, was significantly lower than that in the WT strain ($P < 0.05$) (Fig. 3A). The *fre2*Δ mutant produced significantly higher ferric reductase activity than the WT ($P < 0.05$). When grown in the presence of iron, the ferric reductase activity was downregulated in the WT strain and in most of the *fre*Δ mutants, including the *fre1*Δ to *fre4*Δ and *fre7*Δ strains (Fig. 3A). Compared to the WT, the ferric reductase activities in the *fre1*Δ, *fre3*Δ, *fre4*Δ, *fre7*Δ, and *fre201*Δ mutants were significantly lower under high-iron conditions ($P < 0.05$). However, under these conditions, *fre2*Δ and *fre6*Δ mutants exhibited significantly higher ferric reductase activities than the WT ($P < 0.05$), while the *fre5*Δ mutant had a WT level of ferric reductase activity. Interestingly, the ferric reductase activity in the *fre201*Δ mutant was significantly lower than that in the WT strain ($P < 0.05$), irrespective of the iron levels in the growth medium. This result indicates that Fre201 makes the greatest contribution to overall activity, although in general, ferric reductase activity was detected in all *fre*Δ mutants, suggesting some functional redundancy.

Given that some ferric reductases also have cupric reductase activity (18, 22, 34), we also tested each *fre*Δ deletion strain for this activity. For cupric ion reduction, the WT and *fre*Δ deletion strains were grown in defined LCM without or with 100 μM $CuSO_4$. Under low-copper conditions, the *fre3*Δ to *fre6*Δ mutants produced a WT level of cupric reductase activity (Fig. 3B). However, cupric reductase activity in the *fre1*Δ and *fre7*Δ mutants was lower than that in the WT strain. Under high-copper conditions, the cupric reductase activity was upregulated in all strains, except in the *fre4*Δ, *fre5*Δ, and *fre7*Δ mutants (Fig. 3B). Additionally, in this medium, the *fre4*Δ and *fre7*Δ mutants had significantly lower cupric reductase activity than that in the WT ($P < 0.05$). However, the cupric reductase activity in the *fre2*Δ and *fre201*Δ mutants was significantly higher than that in the WT ($P < 0.05$), irrespective of the copper concentration in the media (Fig. 3B).

Deletion of *FRE4* impaired melanin production. Next, we examined all of the *fre* deletion mutants for virulence-related phenotypes, including their ability to grow at 37°C (host body temperature) and elaboration of the major virulence factors capsule and melanin. These analyses showed that all of the *fre* mutants grew at 37°C and produced capsule similar to the WT strain (data not shown). However, when the *fre*Δ deletion strains were tested on L-DOPA medium for melanin formation, the *fre4*Δ strain showed a defect in melanin biosynthesis (Fig. 4A). Because exogenous copper induces melanin production and laccase activity (a copper-requiring enzyme that catalyzes the conversion of L-DOPA to melanin) and Fre4 could also have cupric reductase activity, we reasoned that the melanin-negative phenotype of the *fre4*Δ strain was due to poor copper availability. To test this hypothesis, the WT and *fre4*Δ strains were grown on L-DOPA plates with 50 μM $CuSO_4$ and also on control plates without $CuSO_4$. Addition of copper restored melanin biosynthesis in the *fre4*Δ strain to a level similar to that in the WT (Fig. 4B). Furthermore, qRT-PCR analysis for *LAC1* (which encodes laccase) expression showed no differences in mRNA expression levels between the mutant and the WT strains (see Fig. S1 in the supplemental material), ruling out a transcriptional effect of Fre4 on *LAC1*.

Fre2 is required for robust growth on hemin and transferrin. To further characterize the functions of the *FRE* genes, we tested the growth of the *fre*Δ mutants on various iron sources *in vitro*. All strains were first grown for 2 days in YNB-LIM to exhaust intracellular iron stores. After iron starvation, we tested growth of all the strains by agar spotting assays on YNB-LIM without or with

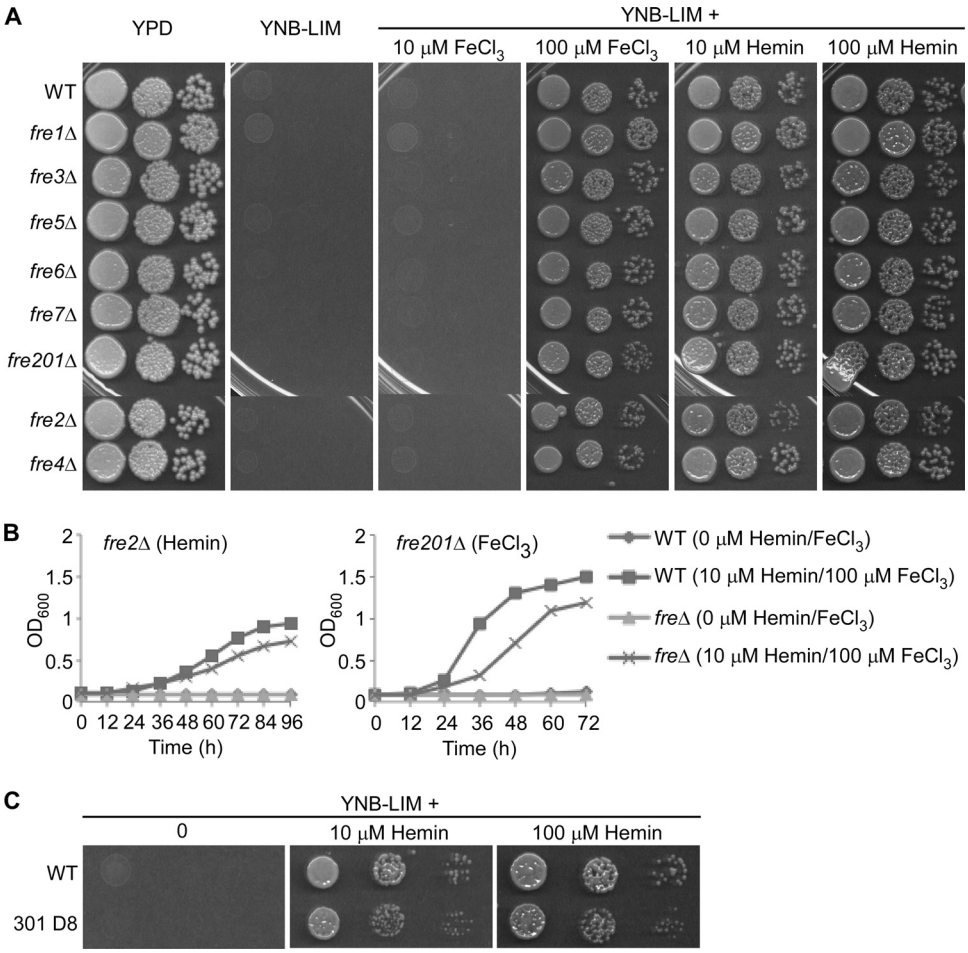

FIG 5 Fre2 is required for robust growth on hemin. Strains were first iron starved in YNB-LIM for 2 days, washed, and then transferred to either solid agar plates or liquid medium. (A) Tenfold serial dilutions of iron-starved strains were spotted on YPD, YNB-LIM, and YNB-LIM with different concentrations of $FeCl_3$ or hemin as indicated. Plates were incubated at 30°C for 2 days. (B) Iron-starved strains were inoculated into YNB-LIM with no iron or with different concentrations of $FeCl_3$ or hemin as indicated. Cultures were incubated at 30°C with shaking, and turbidity was measured every 12 h. Reduced growth of *fre2*Δ and *fre201*Δ mutants was consistently observed in several repeats of the experiments. (C) Tenfold serial dilutions of iron-starved strains were spotted on YNB-LIM and YNB-LIM with different concentrations of hemin as indicated. Plates were incubated at 30°C for 2 days.

$FeCl_3$ or hemin at different concentrations. These spot assays showed that the *fre201*Δ and *fre2*Δ strains had a subtle growth defect in the presence of $FeCl_3$ (at 100 μM) and hemin (at 10 μM), respectively (Fig. 5A). We also carried out YNB-LIM liquid assays for these two deletion strains and confirmed these growth defects, although the phenotypes were more pronounced under these growth conditions (Fig. 5B). This difference may be the result of free iron contaminating the agar in solid medium. Importantly, we also observed that a mutant with a transfer DNA (T-DNA) insertion in *FRE2* had a severe growth defect in the presence of 10 μM hemin (Fig. 5C). This insertion mutant was obtained in a previously reported screen for mutants with reduced growth on hemin, and it had a more obvious growth defect than with the *fre2*Δ strain (35). Interestingly, the *fre2* insertion mutant was generated in the background of a *cfo1*Δ mutant that lacks the ferroxidase of the high-affinity iron uptake system (35). Thus, the difference in the growth defects between the *fre2* T-DNA insertion and deletion mutants indicates that the high-affinity iron uptake system, along with Fre2, makes a contribution to iron acquisition from hemin. The *cfo1*Δ mutant does not have a growth defect on hemin, and this finding therefore highlights the specific contribution of Fre2 (7). The growth defect of the *fre2*Δ strain was overcome by excess hemin (at 100 μM), suggesting the presence of other systems to acquire iron from hemin at higher concentrations.

We also tested the growth of the *fre*Δ mutants on other iron sources using a high-throughput assay in liquid media (see Materials and Methods). The strains were grown in YNB-LIM liquid media without or with various iron sources, including the mammalian host iron source transferrin (10 μM) or the siderophores ferrichrome (10 μM) and enterobactin (5 μM). All of the *fre*Δ mutants grew to a similar level as the WT strain in the presence of the siderophores (data not shown). However, the *fre2*Δ and *fre201*Δ strains showed a subtle growth defect in the presence of transferrin as the sole iron source (Fig. 6).

We selected *FRE2*, along with *FRE4*, for more detailed subsequent analyses because of the hemin phenotype of the *fre2*Δ strain and the melanin-negative phenotype of the *fre4*Δ strain. In addition, these two genes were of interest because they shared a pattern of expression that was distinct from all of the other genes, and they

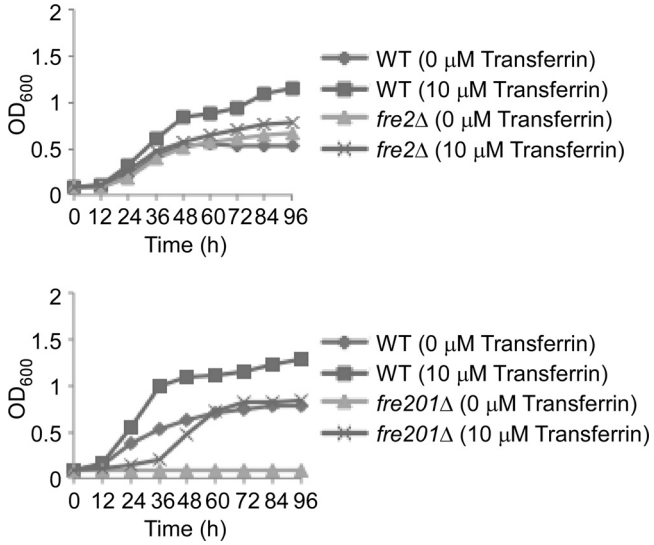

FIG 6 Fre2 and Fre201 are required for robust growth on transferrin. Strains were first iron starved in YNB-LIM for 2 days, washed, and then inoculated into YNB-LIM with no transferrin or with 10 μM transferrin. Cultures were incubated at 30°C with shaking, and turbidity was measured every 12 h. Reduced growth of *fre2*Δ and *fre201*Δ mutants was consistently observed in several repeats of the experiments.

were the only two genes with lower transcript levels in response to hemin. To address potential redundant contributions to reductase activity, we generated double mutants lacking both *FRE2* and *FRE4*. As mentioned above, we also constructed complemented strains wherein a WT copy of *FRE2* or *FRE4* was reintroduced into the single mutants. The *fre2*Δ *fre4*Δ double mutant was also complemented with a WT copy of either *FRE2* (ectopic) or *FRE4* (at the original locus). Although we observed interesting phenotypes for the *fre201*Δ strain, a more detailed analysis of *FRE201* is currently under further investigation. We repeated the growth assays for the *fre2*Δ strain and the complemented strain in the presence of hemin and transferrin. As observed earlier, the *fre2*Δ strain showed less robust growth in the presence of hemin (see Fig. S2 in the supplemental material) and transferrin (see Fig. S3 in the supplemental material). This growth defect in both hemin and transferrin was overcome by the introduction of a WT copy of *FRE2* at the original locus (see Fig. S2 and S3), thus further strengthening the conclusion that Fre2 is required for robust growth on these iron sources. In addition, the melanization defect of the *fre4*Δ strain was reversed by the introduction of a WT copy of *FRE4* at the original locus (see Fig. S4 in the supplemental material).

Fre2 is required for hemin iron acquisition and not for heme uptake. Given that Fre2 had a role in growth on hemin as the sole iron source, we tested whether Fre2 acted as a component of a heme uptake system. That is, it was possible that Fre2 played a role in hemin internalization. To test this hypothesis, we used the noniron metalloporphyrin (MP) Ga-PPIX, which is a toxic heme analog (36). Owing to their structural similarity to heme, MPs enter the cells by a "Trojan horse" mechanism via a heme uptake pathway and act intracellularly to cause toxicity. The WT, *fre2*Δ, and complemented strains were iron starved before comparison of their growth on hemin in the presence or absence of Ga-PPIX. All strains, including the WT, grew well on YPD in the presence or absence of Ga-PPIX suggesting that the heme uptake pathway is not essential under these iron-replete conditions (Fig. 7). However, all of the strains showed weak or no growth on $FeCl_3$ and hemin in the presence of Ga-PPIX, indicating that heme uptake leads to toxicity under these conditions. In addition, all of the strains grew well in the presence of $GaCl_3$, thus attributing the toxic effect to Ga-PPIX and not to gallium. Together, these results demonstrate that loss of Fre2 does not block Ga-PPIX uptake and toxicity and that this candidate reductase therefore probably has no role in heme uptake.

Loss of *FRE4* caused increased susceptibility to antifungal drugs. Previously, a connection between iron availability and antifungal drug susceptibility was observed in *C. neoformans*, *S. cerevisiae*, and *Candida* spp. (7, 8, 37, 38, 39). In *C. neoformans*, loss of *CFO1* and *CFT1* (high-affinity iron uptake components) resulted in increased susceptibility to azole as well as polyene drugs. This phenotype was reversed by exogenous hemin, thus supporting the idea that heme biosynthesis was affected in these mutants, leading to drug susceptibility (7, 8). In this context, we tested the *fre*Δ strains for susceptibility to the antifungal drugs fluconazole, miconazole, and amphotericin B. These drugs are commonly used to treat or reduce the symptoms of cryptococcal meningitis. None of the deletion strains showed altered susceptibility to the polyene antifungal drug amphotericin B (Fig. 8A). However, the *fre4*Δ strain showed increased susceptibility to the azole antifungal drugs fluconazole and miconazole (Fig. 8A). As reported earlier (7, 8), we tested whether this phenotype was related to iron deficiency by studying the response to the drugs in the presence of different iron sources. We found that addition of hemin again reversed the susceptibility to fluconazole (Fig. 8B). Even the addition of inorganic salts $FeCl_3$ and $CuSO_4$ could overcome the susceptibility to the azole drug. These findings are similar to those observed for *C. albicans* iron acquisition mutants (39). Overall, our data suggest that the deletion of *FRE4* resulted in iron deficiency, thereby affecting heme biosynthesis and ultimately affecting ergosterol biosynthesis.

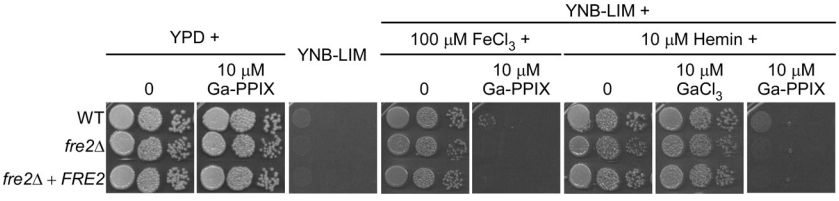

FIG 7 Fre2 is not required for hemin uptake. Strains were first iron starved in YNB-LIM for 2 days, washed, and then transferred to solid agar plates. Tenfold serial dilutions of iron-starved strains were spotted on YPD without or with 10 μM Ga-PPIX, YNB-LIM plus 100 μM $FeCl_3$, or YNB-LIM plus 10 μM hemin without or with 10 μM Ga-PPIX or 10 μM $GaCl_3$ as indicated. Plates were incubated at 30°C for 2 days.

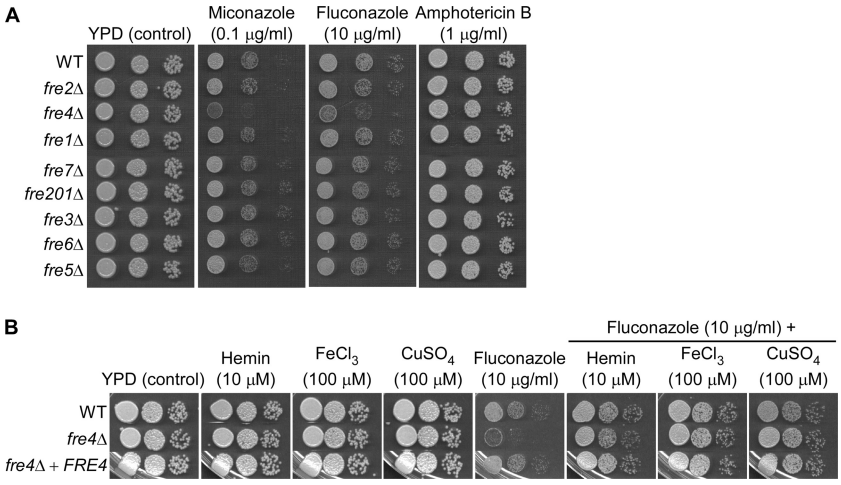

FIG 8 Deletion of *FRE4* increases susceptibility to antifungal drugs. (A) Tenfold serial dilutions of strains were spotted on YPD without or with the antifungal drugs as indicated. Plates were incubated at 30°C for 2 days. (B) Addition of exogenous hemin, $FeCl_3$, or $CuSO_4$ suppressed the antifungal drug susceptibility of the *fre4*Δ mutant. Tenfold serial dilutions of strains were spotted on YPD with fluconazole without or with an iron or copper source as indicated. Plates were incubated at 30°C for 2 days.

Fre2 contributes to virulence in mice. Finally, we tested the virulence of the *fre2*Δ and *fre4*Δ single mutants, the *fre2*Δ *fre4*Δ double mutant and the complemented strains in a mouse inhalation model of cryptococcosis. We tested 13 BALB/c mice per strain for the WT, the *fre2*Δ and *fre4*Δ single mutants and their respective complemented strains, and two independent *fre2*Δ *fre4*Δ double mutants. Of the 13 mice, 3 mice for each strain were used for fungal load analysis at the time that the mice succumbed to infection with the WT strain; the other 10 mice were monitored for the development of disease symptoms. We observed that mice infected with the WT strain, the *fre4*Δ mutant, and the *FRE2* or the *FRE4* complemented strains showed 100% mortality by day 21. However, mice infected with the *fre2*Δ mutant and *fre2*Δ *fre4*Δ double mutants survived to days 26 and 27, respectively (Fig. 9). These results indicate that the deletion of *FRE2*, and *FRE2* in combination with *FRE4*, caused a significant attenuation of virulence, suggesting that Fre2 has a role during infection. Since the *fre2*Δ mutant showed a growth defect in the presence of hemin, we hypothesize that heme iron is important for the growth of *C. neoformans* in mammalian hosts.

We also analyzed the distribution of fungal cells in the lungs and brains of infected mice. Three infected mice for each strain were sacrificed at the same time point (day 20) as the WT-infected mice from the virulence assay (Fig. 9). The numbers of fungal cells in the lungs of mice infected with each strain, except the *fre2*Δ mutant (1 order of magnitude lower than the WT), were comparable. However, the numbers of fungal cells in the brains of mice infected with the *fre2*Δ mutant and the *fre2*Δ *fre4*Δ double mutant were 2 to 4 orders of magnitude lower than those in the brains of mice infected with the WT strain (Fig. 10) suggesting a defect in dissemination and/or colonization of organs. We also noted that the burden for the *fre2*Δ mutant in lungs and brains was lower than the burden for the *fre2*Δ *fre4*Δ double mutants in both tissues. This result suggests that loss of Fre4 improves the ability of

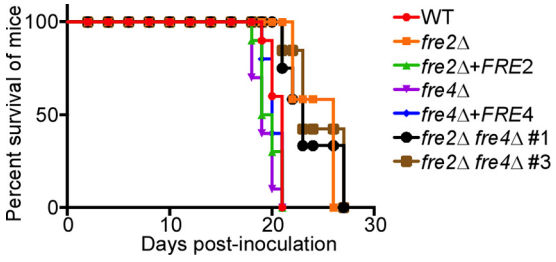

FIG 9 The *fre2*Δ mutant and the *fre2*Δ *fre4*Δ double mutants are attenuated in virulence. Thirteen BALB/c mice were infected intranasally with each of the strains indicated, and the survival of the mice was monitored over the time course indicated on the *x* axis. The difference in survival rates between the *fre2*Δ mutant and the WT strain was significant ($P < 0.0001$), as was the difference between the survival rates of the *fre2*Δ *fre4*Δ double mutants and the WT strain ($P < 0.0001$).

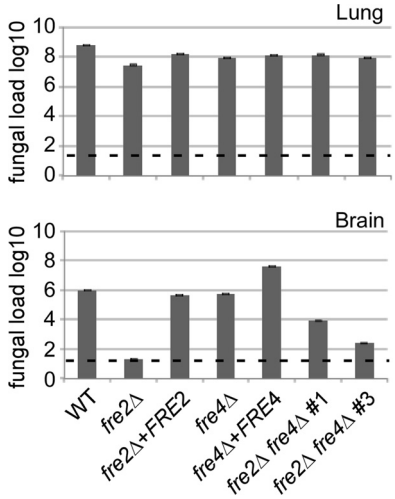

FIG 10 The *fre2*Δ mutant and the *fre2*Δ *fre4*Δ double mutants showed reduced fungal load in the brain in a mouse model of cryptococcosis. The distribution of fungal cells in the lungs and brains of mice was analyzed with three mice for each strain sacrificed at day 20 when WT-infected mice reached the endpoint. The dashed horizontal line indicates the detection limit of the assay, and the error bars indicate standard errors.

the *fre2*Δ mutant to accumulate or persist in the host. Consistent with the fungal load data, the histopathology analysis of the lungs at day 20 of infection showed less abundance of *fre2*Δ mutant cells compared to the WT and *FRE2* complemented strains (see Fig. S5 in the supplemental material).

DISCUSSION

Iron acquisition is critical for the pathogenesis of *C. neoformans*, and there is a well-established role for the reductive, high-affinity uptake system in overall disease and colonization of the central nervous system (5–8, 25, 30, 40, 41). However, the molecular genetics of the enzymatic reduction of ferric to ferrous iron have not been investigated for this pathogen. Ferric reductases are present in all fungal species, with variable numbers predicted across fungal genomes; these enzymes have been studied extensively in *S. cerevisiae* and, to some extent, in *C. albicans*, *S. pombe*, and *A. fumigatus* (13–24, 42). In our study, we identified eight candidate ferric reductase (*FRE*) genes in *C. neoformans*, characterized their expression and contributions to reductase activity, and investigated their roles in virulence factor production. In some fungi, specific reductases account for the majority of the cell-surface reductase activity, and these include *Sc*Fre1p and *Sc*Fre2p in *S. cerevisiae* and *Ca*Fre10 and *Ca*Fre7 in *C. albicans*. For *C. neoformans*, we found that the deletion of individual *FRE* genes did not completely eliminate reductase activity under the conditions tested, although one gene (*FRE201*) made a major contribution. In addition, loss of Fre2 resulted in elevated ferric reductase activity, perhaps due to an influence on iron uptake and intracellular iron levels that resulted in elevated expression of other reductase genes. This result, along with the discoveries of a role for Fre2 in iron acquisition from heme and a contribution of Fre4 to production of the virulence factor melanin, served to focus our attention on these two reductases.

We found that the transcript levels of both *FRE2* and *FRE4* were reduced in the presence of iron and that this reduction was independent of the iron source. Unlike the expression of these two genes, the expression pattern of all the other *FRE* genes was either induced or repressed, depending upon the iron source. Additionally, the transcript level of *FRE4* was strongly repressed in the presence of copper. Based on this observation and the finding that the *fre4*Δ mutant showed reduced cupric reductase activity, we hypothesize that Fre4 may also be a cupric reductase. We also note that a previous study reported upregulation of *FRE7* in *C. neoformans* under low-copper conditions (43). Besides metal regulation, transcription of ferric reductase genes in fungal pathogens is also affected by pH, macrophage engulfment, antifungal drugs, and infection, suggesting distinct regulation of different ferric reductases in response to specific environmental conditions (23, 44–46). These factors remain to be examined in *C. neoformans*, and more detailed interpretation of expression patterns and reductase activities will also require knowledge of the localization of each enzyme.

Our discovery of a role for Fre4 in melanization further supports the possible involvement of this reductase in copper homeostasis. The melanin defect for the *fre4*Δ mutant was not due to the decreased transcription of the *LAC1* gene that encodes the multicopper oxidase (laccase) for melanin production, as similar levels of *LAC1* expression were observed between the mutant and the WT strain. In contrast, addition of copper restored melanin production in the *fre4*Δ mutant, as seen in other melanin-negative or -deficient mutants of *C. neoformans*: e.g., *mel1*, *mel5*, *mel7*, *vph1*, and *clc-a* mutations (47–50). Ferric reductases are also known to reduce copper at the cell surface, as reported in *S. cerevisiae* and *C. albicans* (18, 22, 34). It is therefore possible that Fre4 in *C. neoformans* is a multifunctional enzyme with the ability to reduce copper, and thus its loss resulted in a defect in copper uptake and subsequently affected laccase activity. A defect in copper uptake could also affect the function of additional copper-dependent enzymes in *C. neoformans*. For example, a mutant lacking Sod1 (Cu/Zn superoxide dismutase) is deficient in melanin and also exhibits reduced laccase activity (51). A decrease in ferric/cupric reductase and laccase activities was also observed in the melanin-deficient *oxy2* (copper-sensing transcription factor) mutant and was attributed to the lack of copper (52). Similar observations have been reported in *Podospora anserina*, wherein the loss of the *GRISEA* gene caused a melanin-negative phenotype that was repaired by copper supplementation (53, 54).

We also found that deletion of *FRE4* increased susceptibility to azole drugs, perhaps due to an influence of altered metal homeostasis on iron-dependent ergosterol biosynthesis. Previous studies have also suggested increased membrane fluidity as well as iron deficiency as contributing factors in the increased susceptibility of iron uptake mutants to antifungal drugs (7, 8, 39). For example, the *ftr1* and *ftr2* iron uptake mutants and the *ccc2* copper transporter mutant showed increased susceptibility to the antifungal drug fluconazole in *C. albicans* (39). This susceptibility was overcome by addition of iron. Similarly, the drug susceptibility of *cfo1*Δ and *cft1*Δ mutants in *C. neoformans* was suppressed by addition of hemin, as well as the siderophore deferoxamine (for the *cfo1*Δ mutant) (7, 8). We tested the influence of iron with the *fre4*Δ mutant and found that addition of hemin suppressed the drug susceptibility. We also found that addition of $FeCl_3$ and $CuSO_4$ suppressed the susceptibility of the *fre4*Δ mutant, as observed for the *C. albicans* mutants. It was interesting that the addition of $CuSO_4$ reduced the drug susceptibility of the mutant. We speculate that loss of Fre4 resulted in defective copper acquisition, thereby affecting iron availability. This is because the high-affinity iron uptake component Cfo1 is a copper-requiring enzyme and Fre4 may also be a cupric reductase. A similar role for copper chelation in increasing susceptibility to drugs was observed in *C. albicans* (39). More recently, the heme-binding protein Dap1 in *Candida glabrata* was shown to be required for growth under low-iron conditions and also for azole drug tolerance (38).

Heme and transferrin are both important sources of iron for pathogens during infection of vertebrate hosts. Mechanisms of heme uptake have been well characterized in pathogenic bacteria and involve the recognition of heme or heme-loaded hemophores by surface receptors before delivery to membrane transporters and subsequent internalization (55). Although less is known about the use of heme in parasites and pathogenic fungi, *Leishmania amazonensis* was recently found to have a heme receptor that was required for heme utilization, and the pathogenic fungi *C. albicans* and *Histoplasma capsulatum* utilize heme and/or hemoglobin via cell surface receptors (9, 10, 56, 57). *C. neoformans* also uses heme and hemoglobin as iron sources, and the mannoprotein Cig1 was recently implicated in heme uptake (6). Cig1 shows heme-binding properties, and its loss delayed growth in hemin and reduced susceptibility to noniron metalloporphyrins. In our study, we discovered that Fre2 contributes to heme use by *C. neoformans*. Loss of Fre2 resulted in a subtle growth defect in the

presence of hemin, but unlike Cig1, Fre2 was involved in acquisition of iron from hemin rather than uptake. The *fre2*Δ mutant had a less severe growth defect in hemin than a *cig1*Δ mutant, and this suggests (i) a minor role for the enzyme, (ii) a contribution as part of a cell surface activity involving other components, and (iii) the presence of additional heme utilization systems like the one involving Cig1. Support for Fre2's acting together with other components at the cell surface comes from the observation that loss of both Fre2 and the ferroxidase Cfo1 for high-affinity uptake resulted in a more severe growth defect on hemin than the loss of Fre2 alone. Both ferric reductase and the high-affinity iron uptake system appear to contribute to the use of iron from hemin. Furthermore, the growth defect of the *fre2*Δ mutant was overcome by supplementing the growth medium with excess hemin. This suggests the presence of other systems for acquisition of iron from hemin at higher concentrations. A similar conclusion was recently reported during the analysis of Cig1 (6).

We also observed a role for Fre2 in growth on transferrin, and we note that a role for reductive iron uptake from transferrin has previously been observed in *C. albicans* (12). In that study, *Ca*Fre10 facilitated the reduction and release of iron from transferrin for subsequent uptake by the high-affinity permease-multicopper oxidase system. The contribution of *Ca*Fre10 activity was greater under acidic conditions, and another cell surface reductase, *Ca*Fre1, contributed to reductive transferrin-iron uptake under alkaline conditions (12). Our earlier studies revealed that the reductive, high-affinity iron uptake system (involving Cfo1 and Cft1) was required for iron utilization from transferrin and $FeCl_3$ in *C. neoformans* (7, 8). In the present study, we extended our understanding of this process by identifying the ferric reductases (Fre2 and additionally Fre201) that release transferrin iron for subsequent utilization via the high-affinity reductive system. The contribution of Fre201 in transferrin utilization was comparatively larger than that of Fre2, and the role of Fre201 is currently under further investigation. Analogous to *C. albicans*, we speculate that Fre2 and Fre201 may contribute to the use of iron from transferrin under conditions that are specific for each reductase.

Finally, we analyzed the virulence of the *fre2*Δ, *fre4*Δ, and *fre2*Δ *fre4*Δ mutants using a mouse inhalation model of cryptococcosis and found that Fre2 but not Fre4 contributed to virulence. This result revealed Fre2 as a new component of the iron acquisition mechanisms that impact virulence in *C. neoformans* and, interestingly, indicated that the melanin defect of the *fre4*Δ mutant was not relevant for virulence. An analysis of the fungal burden in infected mice also showed that deletion of *FRE2* impaired the dissemination of the mutant from lungs to the brain and/or colonization of the brain. This defect is reminiscent of the reduced fungal burden observed for mutants lacking the Cft1 and Cfo1 components of the high-affinity uptake system in *C. neoformans* (6, 7, 8). Since the *fre2*Δ mutant showed a defect in the use of hemin as an iron source, it is likely that hemin may be important for the growth of *C. neoformans* during infection. It was also interesting that deletion of *FRE4* improved the ability of the *fre2*Δ mutant to accumulate or persist in the brains and lungs of infected mice. This result suggests the potential for complex interactions between reductases and possible competing contributions to metal homeostasis. In general, the identification of a role of ferric reductases in cryptococcal virulence is a novel finding for fungal pathogens of humans. Ferric reductases have been characterized in *C. albicans* and *A. fumigatus*, but none of these enzymes have so far been implicated in virulence (13, 22, 23, 46). For *C. neoformans*, additional work is needed to understand the interactions between reductases, the contributions of each of the enzymes to virulence, and the mechanisms by which Fre2 participates in iron use from heme and transferrin.

ACKNOWLEDGMENTS

This research was supported by a grant from the National Institute of Allergy and Infectious Diseases (RO1 AI053721). J.K. gratefully acknowledges a Scholar Award in Molecular Pathogenic Mycology from the Burroughs Wellcome Fund. D.O. was supported by a grant from CNPq, Brazil.

We acknowledge Wax-it Histology Services, Inc., for participating in the histopathology experiment.

REFERENCES

1. **Hissen AH, Wan AN, Warwas ML, Pinto LJ, Moore MM.** 2005. The *Aspergillus fumigatus* siderophore biosynthetic gene *sidA*, encoding L-ornithine N5-oxygenase, is required for virulence. Infect. Immun. **73:**5493–5503. http://dx.doi.org/10.1128/IAI.73.9.5493-5503.2005.
2. **Schrettl M, Bignell E, Kragl C, Joechl C, Rogers T, Arst HN, Jr, Haynes K, Haas H.** 2004. Siderophore biosynthesis but not reductive iron assimilation is essential for *Aspergillus fumigatus* virulence. J. Exp. Med. **200:**1213–1219. http://dx.doi.org/10.1084/jem.20041242.
3. **Schrettl M, Bignell E, Kragl C, Sabiha Y, Loss O, Eisendle M, Wallner A, Arst HN, Jr, Haynes K, Haas H.** 2007. Distinct roles for intra- and extracellular siderophores during *Aspergillus fumigatus* infection. PLoS Pathog. **3:**1195–1207. http://dx.doi.org/10.1371/journal.ppat.0030128.
4. **Heymann P, Gerads M, Schaller M, Dromer F, Winkelmann G, Ernst JF.** 2002. The siderophore iron transporter of *Candida albicans* (Sit1p/Arn1p) mediates uptake of ferrichrome-type siderophores and is required for epithelial invasion. Infect. Immun. **70:**5246–5255. http://dx.doi.org/10.1128/IAI.70.9.5246-5255.2002.
5. **Tangen KL, Jung WH, Sham AP, Lian T, Kronstad JW.** 2007. The iron- and cAMP-regulated gene *SIT1* influences ferrioxamine B utilization, melanization and cell wall structure in *Cryptococcus neoformans*. Microbiology **153:**29–41. http://dx.doi.org/10.1099/mic.0.2006/000927-0.
6. **Cadieux B, Lian T, Hu G, Wang J, Biondo C, Teti G, Liu V, Murphy ME, Creagh AL, Kronstad JW.** 2013. The mannoprotein Cig1 supports iron acquisition from heme and virulence in the pathogenic fungus *Cryptococcus neoformans*. J. Infect. Dis. **207:**1339–1347. http://dx.doi.org/10.1093/infdis/jit029.
7. **Jung WH, Hu G, Kuo W, Kronstad JW.** 2009. Role of ferroxidases in iron uptake and virulence of *Cryptococcus neoformans*. Eukaryot. Cell **8:**1511–1520. http://dx.doi.org/10.1128/EC.00166-09.
8. **Jung WH, Sham A, Lian T, Singh A, Kosman DJ, Kronstad JW.** 2008. Iron source preference and regulation of iron uptake in *Cryptococcus neoformans*. PLoS Pathog. **4:**e45. http://dx.doi.org/10.1371/journal.ppat.0040045.
9. **Santos R, Buisson N, Knight S, Dancis A, Camadro JM, Lesuisse E.** 2003. Haemin uptake and use as an iron source by *Candida albicans*: role of *CaHMX1*-encoded haem oxygenase. Microbiology **149:**579–588. http://dx.doi.org/10.1099/mic.0.26108-0.
10. **Weissman Z, Kornitzer D.** 2004. A family of *Candida* cell surface haem-binding proteins involved in haemin and haemoglobin-iron utilization. Mol. Microbiol. **53:**1209–1220. http://dx.doi.org/10.1111/j.1365-2958.2004.04199.x.
11. **Weissman Z, Shemer R, Conibear E, Kornitzer D.** 2008. An endocytic mechanism for haemoglobin-iron acquisition in *Candida albicans*. Mol. Microbiol. **69:**201–217. http://dx.doi.org/10.1111/j.1365-2958.2008.06277.x.
12. **Knight SA, Vilaire G, Lesuisse E, Dancis A.** 2005. Iron acquisition from transferrin by *Candida albicans* depends on the reductive pathway. Infect. Immun. **73:**5482–5492. http://dx.doi.org/10.1128/IAI.73.9.5482-5492.2005.
13. **Blatzer M, Binder U, Haas H.** 2011. The metalloreductase FreB is involved in adaptation of *Aspergillus fumigatus* to iron starvation. Fungal Genet. Biol. **48:**1027–1033. http://dx.doi.org/10.1016/j.fgb.2011.07.009.
14. **Hammacott JE, Williams PH, Cashmore AM.** 2000. *Candida albicans CFL1* encodes a functional ferric reductase activity that can rescue a *Saccharomyces cerevisiae fre1* mutant. Microbiology **146:**869–876. http://mic.sgmjournals.org/content/146/4/869.long

15. **Knight SA, Lesuisse E, Stearman R, Klausner RD, Dancis A.** 2002. Reductive iron uptake by *Candida albicans*: role of copper, iron and the *TUP1* regulator. Microbiology **148:**29–40. http://mic.sgmjournals.org/content/148/1/29.long.
16. **Philpott CC, Protchenko O.** 2008. Response to iron deprivation in *Saccharomyces cerevisiae*. Eukaryot. Cell **7:**20–27. http://dx.doi.org/10.1128/EC.00354-07.
17. **Roman DG, Dancis A, Anderson GJ, Klausner RD.** 1993. The fission yeast ferric reductase gene *frp1*$^+$ is required for ferric iron uptake and encodes a protein that is homologous to the gp91-*phox* subunit of the human NADPH phagocyte oxidoreductase. Mol. Cell. Biol. **13:**4342–4350.
18. **Georgatsou E, Mavrogiannis LA, Fragiadakis GS, Alexandraki D.** 1997. The yeast Fre1p/Fre2p cupric reductases facilitate copper uptake and are regulated by the copper-modulated Mac1p activator. J. Biol. Chem. **272:**13786–13792. http://dx.doi.org/10.1074/jbc.272.21.13786.
19. **Yun CW, Bauler M, Moore RE, Klebba PE, Philpott CC.** 2001. The role of the *FRE* family of plasma membrane reductases in the uptake of siderophore-iron in *Saccharomyces cerevisiae*. J. Biol. Chem. **276:**10218–10223. http://dx.doi.org/10.1074/jbc.M010065200.
20. **Georgatsou E, Alexandraki D.** 1999. Regulated expression of the *Saccharomyces cerevisiae* Fre1p/Fre2p Fe/Cu reductase related genes. Yeast **15:**573–584. http://dx.doi.org/10.1002/(SICI)1097-0061(199905)15:7<573::AID-YEA404>3.0.CO;2-7.
21. **Martins LJ, Jensen LT, Simon JR, Keller GL, Winge DR.** 1998. Metalloregulation of *FRE1* and *FRE2* homologs in *Saccharomyces cerevisiae*. J. Biol. Chem. **273:**23716–23721. http://dx.doi.org/10.1074/jbc.273.37.23716.
22. **Jeeves RE, Mason RP, Woodacre A, Cashmore AM.** 2011. Ferric reductase genes involved in high-affinity iron uptake are differentially regulated in yeast and hyphae of *Candida albicans*. Yeast **28:**629–644. http://dx.doi.org/10.1002/yea.1892.
23. **Baek YU, Li M, Davis DA.** 2008. *Candida albicans* ferric reductases are differentially regulated in response to distinct forms of iron limitation by the Rim101 and CBF transcription factors. Eukaryot. Cell **7:**1168–1179. http://dx.doi.org/10.1128/EC.00108-08.
24. **Woodacre A, Mason RP, Jeeves RE, Cashmore AM.** 2008. Copper-dependent transcriptional regulation by *Candida albicans* Mac1p. Microbiology **154:**1502–1512. http://dx.doi.org/10.1099/mic.0.2007/013441-0.
25. **Lian T, Simmer MI, D'Souza CA, Steen BR, Zuyderduyn SD, Jones SJ, Marra MA, Kronstad JW.** 2005. Iron-regulated transcription and capsule formation in the fungal pathogen *Cryptococcus neoformans*. Mol. Microbiol. **55:**1452–1472. http://dx.doi.org/10.1111/j.1365-2958.2004.04474.x.
26. **Vartivarian SE, Anaissie EJ, Cowart RE, Sprigg HA, Tingler MJ, Jacobson ES.** 1993. Regulation of cryptococcal capsular polysaccharide by iron. J. Infect. Dis. **167:**186–190. http://dx.doi.org/10.1093/infdis/167.1.186.
27. **Davidson RC, Blankenship JR, Kraus PR, de Jesus Berrios M, Hull CM, D'Souza C, Wang P, Heitman J.** 2002. A PCR-based strategy to generate integrative targeting alleles with large regions of homology. Microbiology **148:**2607–2615. http://mic.sgmjournals.org/content/148/8/2607.long.
28. **Yu JH, Hamari Z, Han KH, Seo JA, Reyes-Dominguez Y, Scazzocchio C.** 2004. Double-joint PCR: a PCR-based molecular tool for gene manipulations in filamentous fungi. Fungal Genet. Biol. **41:**973–981. http://dx.doi.org/10.1016/j.fgb.2004.08.001.
29. **Toffaletti DL, Rude TH, Johnston SA, Durack DT, Perfect JR.** 1993. Gene transfer in *Cryptococcus neoformans* by use of biolistic delivery of DNA. J. Bacteriol. **175:**1405–1411.
30. **Jung WH, Saikia S, Hu G, Wang J, Fung CK, D'Souza C, White R, Kronstad JW.** 2010. HapX positively and negatively regulates the transcriptional response to iron deprivation in *Cryptococcus neoformans*. PLoS Pathog. **6:**e1001209. http://dx.doi.org/10.1371/journal.ppat.1001209.
31. **Livak KJ, Schmittgen TD.** 2001. Analysis of relative gene expression data using real-time quantitative PCR and the $2^{-\Delta\Delta CT}$ method. Methods **25:**402–408. http://dx.doi.org/10.1006/meth.2001.1262.
32. **Nyhus KJ, Jacobson ES.** 1999. Genetic and physiologic characterization of ferric/cupric reductase constitutive mutants of *Cryptococcus neoformans*. Infect. Immun. **67:**2357–2365.
33. **Zhang X, Krause KH, Xenarios I, Soldati T, Boeckmann B.** 2013. Evolution of the ferric reductase domain (FRD) superfamily: modularity, functional diversification, and signature motifs. PLoS One **8:**e58126. http://dx.doi.org/10.1371/journal.pone.0058126.
34. **Hassett R, Kosman DJ.** 1995. Evidence for Cu(II) reduction as a component of copper uptake by *Saccharomyces cerevisiae*. J. Biol. Chem. **270:**128–134. http://dx.doi.org/10.1074/jbc.270.1.128.
35. **Hu G, Caza M, Cadieux B, Chan V, Liu V, Kronstad J.** 2013. *Cryptococcus neoformans* requires the ESCRT protein Vps23 for iron acquisition from heme, for capsule formation, and for virulence. Infect. Immun. **81:**292–302. http://dx.doi.org/10.1128/IAI.01037-12.
36. **Stojiljkovic I, Kumar V, Srinivasan N.** 1999. Non-iron metalloporphyrins: potent antibacterial compounds that exploit haem/Hb uptake systems of pathogenic bacteria. Mol. Microbiol. **31:**429–442. http://dx.doi.org/10.1046/j.1365-2958.1999.01175.x.
37. **Barker KS, Pearson MM, Rogers PD.** 2003. Identification of genes differentially expressed in association with reduced azole susceptibility in *Saccharomyces cerevisiae*. J. Antimicrob. Chemother. **51:**1131–1140. http://dx.doi.org/10.1093/jac/dkg217.
38. **Hosogaya N, Miyazaki T, Nagi M, Tanabe K, Minematsu A, Nagayoshi Y, Yamauchi S, Nakamura S, Imamura Y, Izumikawa K, Kakeya H, Yanagihara K, Miyazaki Y, Kugiyama K, Kohno S.** 2013. The heme-binding protein Dap1 links iron homeostasis to azole resistance via the P450 protein Erg11 in *Candida glabrata*. FEMS Yeast Res. **13:**411–421. http://dx.doi.org/10.1111/1567-1364.12043.
39. **Prasad T, Chandra A, Mukhopadhyay CK, Prasad R.** 2006. Unexpected link between iron and drug resistance of *Candida* spp.: iron depletion enhances membrane fluidity and drug diffusion, leading to drug-susceptible cells. Antimicrob. Agents Chemother. **50:**3597–3606. http://dx.doi.org/10.1128/AAC.00653-06.
40. **Barluzzi R, Saleppico S, Nocentini A, Boelaert JR, Neglia R, Bistoni F, Blasi E.** 2002. Iron overload exacerbates experimental meningoencephalitis by *Cryptococcus neoformans*. J. Neuroimmunol. **132:**140–146. http://dx.doi.org/10.1016/S0165-5728(02)00324-7.
41. **Jung WH, Sham A, White R, Kronstad JW.** 2006. Iron regulation of the major virulence factors in the AIDS-associated pathogen *Cryptococcus neoformans*. PLoS Biol. **4:**e410. http://dx.doi.org/10.1371/journal.pbio.0040410.
42. **Grissa I, Bidard F, Grognet P, Grossetete S, Silar P.** 2010. The Nox/ferric reductase/ferric reductase-like families of Eumycetes. Fungal Biol. **114:**766–777. http://dx.doi.org/10.1016/j.funbio.2010.07.002.
43. **Ding C, Yin J, Tovar EM, Fitzpatrick DA, Higgins DG, Thiele DJ.** 2011. The copper regulon of the human fungal pathogen *Cryptococcus neoformans* H99. Mol. Microbiol. **81:**1560–1576. http://dx.doi.org/10.1111/j.1365-2958.2011.07794.x.
44. **Lee RE, Liu TT, Barker KS, Rogers PD.** 2005. Genome-wide expression profiling of the response to ciclopirox olamine in *Candida albicans*. J. Antimicrob. Chemother. **55:**655–662. http://dx.doi.org/10.1093/jac/dki105.
45. **Lorenz MC, Bender JA, Fink GR.** 2004. Transcriptional response of *Candida albicans* upon internalization by macrophages. Eukaryot. Cell **3:**1076–1087. http://dx.doi.org/10.1128/EC.3.5.1076-1087.2004.
46. **McDonagh A, Fedorova ND, Crabtree J, Yu Y, Kim S, Chen D, Loss O, Cairns T, Goldman G, Armstrong-James D, Haynes K, Haas H, Schrettl M, May G, Nierman WC, Bignell E.** 2008. Sub-telomere directed gene expression during initiation of invasive aspergillosis. PLoS Pathog. **4:**e1000154. http://dx.doi.org/10.1371/journal.ppat.1000154.
47. **Torres-Guererro H, Edman JC.** 1994. Melanin-deficient mutants of *Cryptococcus neoformans*. J. Med. Vet. Mycol. **32:**303–313. http://dx.doi.org/10.1080/02681219480000381.
48. **Zhu X, Gibbons J, Zhang S, Williamson PR.** 2003. Copper-mediated reversal of defective laccase in a Δ*vph1* avirulent mutant of *Cryptococcus neoformans*. Mol. Microbiol. **47:**1007–1014. http://dx.doi.org/10.1046/j.1365-2958.2003.03340.x.
49. **Zhu X, Williamson PR.** 2003. A CLC-type chloride channel gene is required for laccase activity and virulence in *Cryptococcus neoformans*. Mol. Microbiol. **50:**1271–1281. http://dx.doi.org/10.1046/j.1365-2958.2003.03752.x.
50. **Zhu X, Williamson PR.** 2004. Role of laccase in the biology and virulence of *Cryptococcus neoformans*. FEMS Yeast Res. **5:**1–10. http://dx.doi.org/10.1016/j.femsyr.2004.04.004.
51. **Narasipura SD, Ault JG, Behr MJ, Chaturvedi V, Chaturvedi S.** 2003. Characterization of Cu, Zn superoxide dismutase (*SOD1*) gene knock-out mutant of *Cryptococcus neoformans var. gattii*: role in biology and virulence. Mol. Microbiol. **47:**1681–1694. http://dx.doi.org/10.1046/j.1365-2958.2003.03393.x.

52. **Nyhus K, Jacobson ES.** 2004. *Oxy2* as a transcriptional activator gene for copper uptake in *Cryptococcus neoformans*. Med. Mycol. **42:**325–331. http://dx.doi.org/10.1080/13693780310001658757.
53. **Borghouts C, Osiewacz HD.** 1998. GRISEA, a copper-modulated transcription factor from *Podospora anserina* involved in senescence and morphogenesis, is an ortholog of MAC1 in *Saccharomyces cerevisiae*. Mol. Gen. Genet. **260:**492–502. http://dx.doi.org/10.1007/s004380050922.
54. **Marbach K, Fernandez-Larrea J, Stahl U.** 1994. Reversion of a long-living, undifferentiated mutant of *Podospora anserina* by copper. Curr. Genet. **26:**184–186. http://dx.doi.org/10.1007/BF00313809.
55. **Smith AD, Wilks A.** 2012. Extracellular heme uptake and the challenges of bacterial cell membranes. Curr. Top. Membr. **69:**359–392. http://dx.doi.org/10.1016/B978-0-12-394390-3.00013-6.
56. **Foster LA.** 2002. Utilization and cell-surface binding of hemin by *Histoplasma capsulatum*. Can. J. Microbiol. **48:**437–442. http://dx.doi.org/10.1139/w02-037.
57. **Huynh C, Yuan X, Miguel DC, Renberg RL, Protchenko O, Philpott CC, Hamza I, Andrews NW.** 2012. Heme uptake by *Leishmania amazonensis* is mediated by the transmembrane protein LHR1. PLoS Pathog. **8:**e1002795. http://dx.doi.org/10.1371/journal.ppat.1002795.